Appl. Phys. A 69 [Suppl.], S75–S80 (1999) / Digital Object Identifier (DOI) 10.1007/s003399900347

**Applied Physics A**
Materials
Science & Processing


# Mechanisms of laser ablation from molecular dynamics simulations: dependence on the initial temperature and pulse duration

**L.V. Zhigilei, B.J. Garrison**

Department of Chemistry, 152 Davey Laboratory, The Pennsylvania State University, University Park, PA 16802, USA
(Fax: +1-814/863-5319, E-mail: leo@chem.psu.edu)

Received: 1 July 1999/Accepted: 15 September 1999/Published online: 22 December 1999

**Abstract.** The effect of the initial sample temperature and laser pulse duration on the mechanisms of molecular ejection from an irradiated molecular solid is investigated by large-scale molecular dynamics simulations. The results of simulations performed for two initial temperatures are found to be consistent with the notion of two distinct regimes of molecular ejection separated by a threshold fluence. At low laser fluences, thermal desorption from the surface is observed and the desorption yield is described by an Arrhenius-type dependence on the laser fluence. At fluences above the threshold, a collective multilayer ejection or ablation occurs and the ablation depth follows a critical density of the deposited energy. The same activation energy for desorption and critical energy density for ablation provide a good description of the fluence dependence of the total yield in simulations with different initial temperatures. Comparison of the simulation results for two pulse durations is performed to elucidate the differences in the ejection mechanisms in the regimes of thermal and stress confinement. We find that in the regime of stress confinement, high thermoelastic pressure can cause mechanical fracture/cavitation leading to energetically efficient ablation and ejection of large relatively cold chunks of material.

**PACS:** 61.80.Az; 02.70.Ns; 79.20.Ds

The need to understand the mechanisms of laser ablation of organic solids is defined by a rapid expansion in the practical applications of this phenomenon. In particular, laser ablation is used for controlled removal of biological tissue in laser surgery [1, 2], for desorption/ionization of biomolecules in mass-spectrometric investigations [2–6], and for surface microfabrication of polymer films [7, 8]. Despite active application and intense experimental and theoretical studies, a complete understanding of the physical processes leading to the material removal is still lacking.

Recent results of molecular dynamics (MD) simulations have demonstrated the potential of this technique for the detailed investigation of the mechanisms of laser ablation. For molecular systems, the atomic-level picture of disruption of the hydrogen bonds [9] and the dynamics of intermolecular redistribution of the deposited laser energy [10, 11] have been studied. The direct application of the atomistic MD approach to the laser ablation phenomenon, however, is hampered by the collective character of the processes involved occurring at the mesoscopic rather than the molecular scale. Recent development of a coarse-grained breathing sphere MD model, where a group of atoms, rather then each atom, is treated as a unit, has significantly expanded the time and length scales accessible for the simulations [12]. The model not only allows one to perform simulations with irradiation parameters comparable to the experimental values [13], but it also permits a translation of microscopic information on the dynamics of individual molecules into a mesoscopic description of the laser-induced processes in terms of temperature, pressure and energy distributions within the irradiated sample [12–16]. This, in turn, has allowed us to define different regimes of molecular ejection and to propose a consistent analytical description of the yield dependence on the laser fluence [13].

The analysis of the mechanisms of molecular ejection and the description of the yield vs. fluence dependence proposed in [13] is based on the results of simulations performed for a model sample with zero initial temperature. In our work we test the conclusions derived from the simulations with zero initial temperature by performing a series of simulations for samples that are preheated and equilibrated at 500 K before irradiation with a laser pulse. Simulation results are related to recent mass spectrometry data from Schürenberg et al. on the effect of the sample temperature on the yield of molecular ions and postionized neutral molecules [5]. Although in [5] the experimental data is discussed in the framework of a quasi-thermal desorption model [3], the results of the simulations for two initial temperatures, presented in Sect. 2.1 of this paper, suggest an alternative interpretation.

Another parameter that has a strong influence on the ejection process is the laser pulse duration. In Sect. 2.2 we report preliminary results on the dependence of the mechanisms of material ejection on pulse duration. The ejection mechan-

COLA'99 – 5th International Conference on Laser Ablation, July 19–23, 1999 in Göttingen, Germany

isms are compared for two series of MD simulations with the values for the laser penetration depth and pulse duration chosen so that the regime of stress confinement is realized in one set of the simulations and the regime of thermal confinement is achieved in another. A short discussion of the overall picture emerging from the large-scale simulations of laser ablation with different pulse durations and initial sample temperatures is given in Sect. 3.

## 1 Computational setup

In this section we briefly review the basic features of the breathing sphere model developed for MD simulation of laser ablation of organic solids and describe the computational setup used in our study. Complete details of the breathing sphere model are given in [12].

The model assumes that each molecule (or appropriate group of atoms) can be represented by a single particle. The parameters of interparticle interaction are chosen to reproduce the properties of an organic material, in this case a molecular solid. In order to simulate molecular excitation by photon absorption and vibrational relaxation of the excited molecules, an additional internal degree of freedom is attributed to each molecule. This internal degree of freedom, or breathing mode, is realized by allowing the particles to change their sizes. The parameters of a potential function ascribed to the internal motion can be used to change the characteristic frequency of the breathing mode and to affect the coupling between internal and translational molecular motions. In effect one can control the rate of the conversion of internal energy of the molecules excited by the laser to the translational and internal motion of the other molecules. The rate of the vibrational relaxation of excited molecules is an input parameter in the model and has a time constant of 15 ps in the simulations presented in this paper.

Since in this model each molecule is represented by a single particle, the system size can be large enough to reproduce the collective dynamics leading to laser ablation and damage. Moreover, since explicit atomic vibrations are not followed, the time-step in the numerical integration of the equations of motion can be much longer and the dynamics in the irradiated sample can be followed for as long as nanoseconds.

The system chosen to model the laser ablation is a molecular solid or matrix used in matrix-assisted laser desorption ionization (MALDI) mass spectrometry experiments. The parameters of the intermolecular potential are chosen to represent the van der Waals interaction in a molecular solid with the cohesive energy of 0.6 eV, elastic bulk modulus of $\sim 5$ GPa, and density of $1.2\,\mathrm{g/cm^3}$. A mass of 100 daltons is attributed to each molecule. Most of the results are obtained by using a computational cell of dimensions $10 \times 10 \times 100$ nm (70 526 molecules). A few test simulations with larger computational cells, $20 \times 10 \times 100$ nm (141 052 molecules) and $10 \times 10 \times 180$ nm (126 950 molecules), are done in order to make certain that the simulation results are not affected by the finite size of the computational cell. Periodic boundary conditions in the directions parallel to the surface are imposed. These conditions simulate the situation in which the laser spot diameter is large compared to the penetration depth so that the effects of the edges of the laser beam are neglected. At the bottom of the MD computational cell we apply the dynamic boundary condition developed to avoid artifacts due to reflection of the laser-induced pressure wave from the boundary of the computational cell. The boundary condition accounts for the laser-induced pressure wave propagation as well as the direct laser energy deposition in the boundary region and is described in [16, 17].

The laser irradiation is simulated by vibrational excitation of molecules that are randomly chosen during the laser pulse duration within the penetration depth appropriate for a given wavelength. Vibrational excitation is modeled by depositing a quantum of energy equal to the photon energy into the kinetic energy of the internal motion of a given molecule. Irradiation at a wavelength of 337 nm (3.68 eV) is simulated in this study. The total number of photons entering the model during the laser pulse is determined by the laser fluence, i.e., the incident laser energy per unit surface area. The absorption probability is modulated by Lambert–Beer's law to reproduce the exponential attenuation of the laser light with depth. The absorption depth used in the simulations, 50 nm, is in the range of the values appropriate for strongly absorbing matrixes used in ultra-violet (UV) MALDI.

The value of the laser pulse duration, $\tau_p = 150$ ps, is used in a simulation study of the effect of the initial sample temperature on the ejection process. The pulse duration of 150 ps is short relative to the characteristic thermal diffusion time across the absorption depth, $\tau_{th} \sim 10$ ns, but longer than the time of mechanical equilibration of the absorbing volume, $\tau_s \sim 20$ ps. Thus, the simulations with 150 ps pulses are performed in the regime of thermal confinement ($\tau_p < \tau_{th}$) but not thermo-elastic stress confinement ($\tau_p > \tau_s$). This regime is also characteristic for UV MALDI conditions [3]. It has been demonstrated recently by Dreisewerd et al. [4] that in the regime of thermal confinement the amount of energy deposited by the laser pulse rather than the pulse duration determines the desorption/ablation process. Therefore, even though the pulse duration of 150 ps is an order of magnitude shorter than the durations commonly used in MALDI, a qualitative comparison between the simulation results and UV MALDI experimental data is justified.

In order to investigate the dependence of the ejection mechanisms on the pulse duration we compare simulation results for 150-ps pulses with the results for 15-ps pulses, for which the condition for stress confinement, $\tau_p \leq \tau_s$, is satisfied. The results from this set of simulations can help in the understanding of the microscopic mechanisms responsible for energetically efficient ablation in a number of applications, such as infra-red (IR) MALDI and laser surgery, where the regime of stress confinement is realized [18–20].

## 2 Results

### *2.1 Mechanisms of laser ablation and yield vs. fluence dependence for different initial temperatures of the sample*

Recent results of MD simulation studies of the mechanisms of laser ablation have demonstrated that there are two distinct regimes of molecular ejection separated by a well- defined threshold fluence [12–14]. The existence of two regimes is apparent in the yield–fluence dependence shown in Fig. 1a.

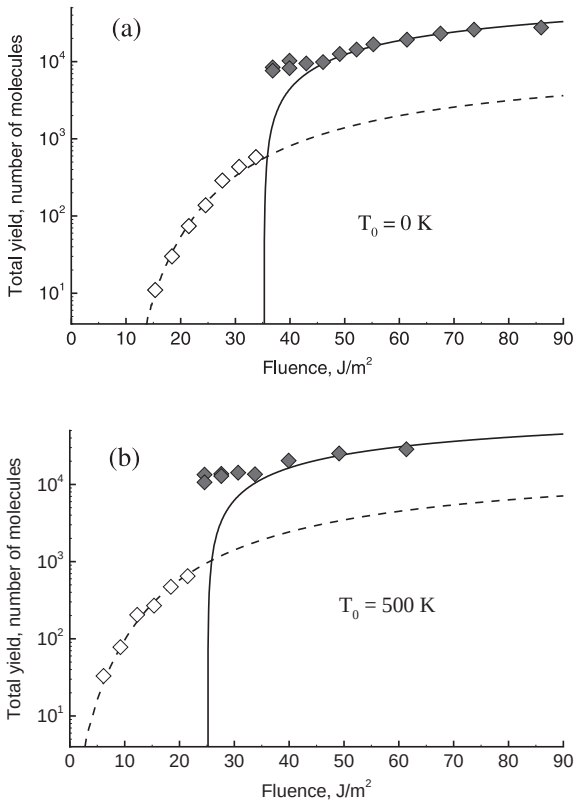


**Fig. 1a,b.** Total yield as a function of laser fluence for simulations with two different initial temperatures of the sample, **a** $T_0 = 0$ K and **b** $T_0 = 500$ K. The *open* and *closed symbols* show the data points below and above the threshold for ablation. The *solid lines* represent prediction of the ablation model (2). The *dashed lines* represent fits of the data points below the threshold to the thermal desorption model (1). The same activation energies, $E_s^* = 0.46$ eV in (1) and $E_v^* = 0.6$ eV in (2) are used for both sets of the simulations. A logarithmic scale is used for better presentation of low fluence data

At low fluences, the yield of ejected molecules is relatively low and the dependence of the number of ejected molecules $N$ on fluence $F$ can be well described by an Arrhenius-type expression

$$N = A \exp\left[-\frac{E_s^*}{k_B(T_0 + BF)}\right] \quad \text{for } F < F_{th}\,, \tag{1}$$

where $E_s^*$ is an activation energy, $A$ is a pre-exponential or frequency factor, $B$ is a factor that describes the conversion of the deposited energy into an increase in the temperature of the surface, $T_0$ is the initial temperature of the sample, $k_B$ is Boltzmann's constant, and $F_{th}$ is an threshold fluence for the onset of a collective material ejection or ablation. As shown in Fig. 1a, (1) with activation energy $E_s^* = 0.46$ eV provides a good fit to the yield–fluence dependence in the low-fluence regime. Mostly monomers are ejected in this regime and the maximum number of molecules ejected at 34 J/m$^2$, right below the threshold fluence, corresponds to only a 0.8-nm layer of the original sample. The thermal desorption model thus provides an adequate description of the molecular ejection at low laser fluences.

As can be seen in Fig. 1a, the total amount of the ejected material increases at the threshold fluence by more then an order of magnitude. The number of molecules ejected at 37 J/m$^2$, right above the threshold fluence, corresponds to a 11.4-nm layer of the original sample. This stepwise transition from ejection of about a monolayer of molecules to a collective ejection, or ablation, of a significant part of the absorbing volume reflects qualitative changes in the ejection mechanism. A series of snapshots from a simulation in the ablation regime is shown in Fig. 2. We observe a homogeneous expansion of a significant part of the absorbing volume followed by decomposition of the ejected plume into gas-phase molecules and liquid droplets. Ejection of large molecular clusters is a distinctive characteristic of the ablation.

The thermal desorption model is not valid in the ablation regime and different analytical description of the yield–fluence dependence should be used. We have found that the amount of ejected material can be relatively well described by a simple model in which the ablation depth follows the laser energy deposition and all material that absorbs an energy density higher than a critical energy density, $E_v^*$, is ablated [13]. With the exponential decay of laser intensity given by Lambert–Beer's law, the total number of molecules ejected per unit surface area is

$$N_{tot} = n_m L_p \ln\left[\frac{F}{L_p(E_v^* - CT_0)}\right] \quad \text{for} \quad F \geq F_{th} = L_p(E_v^* - CT_0)\,, \tag{2}$$

where $n_m$ is the molecular number density of the material, $L_p$ is the laser penetration depth, and $C$ is a specific heat capacity of the model material. This expression predicts the existence of the threshold fluence $F_{th} = L_p(E_v^* - CT_0)$ at which

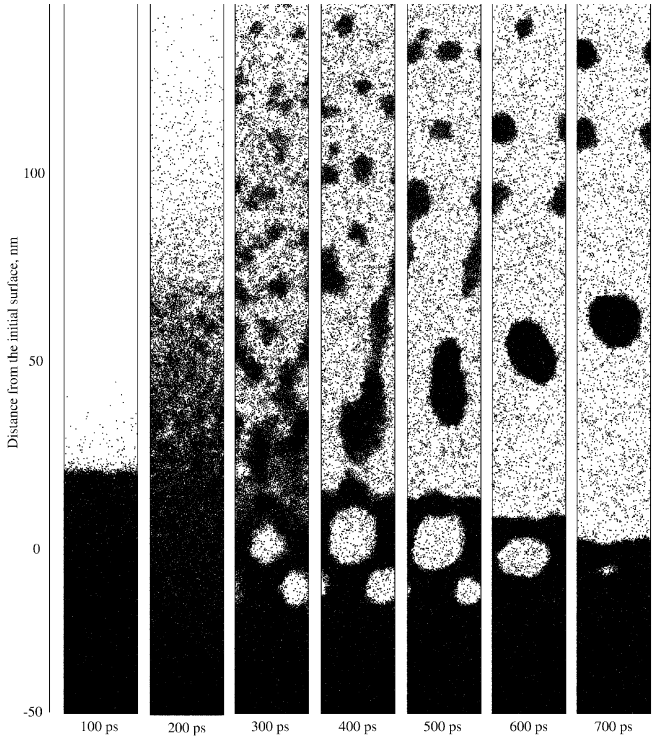


**Fig. 2.** A typical series of snapshots from the simulation in the ablation regime. The laser pulse duration is 150 ps, fluence is 55 J/m$^2$, and penetration depth is 50 nm. An animated sequence of the snapshots for this simulation can be found at http://galilei.chem.psu.edu/ ~leo/Ablation.html

the critical energy density $E_v^*$ is reached in the surface layer. Explosive vaporization of the overheated material has been identified to be a major mechanism of material ejection in this irradiation regime [12–14, 21].

The initial temperature of the sample appears as a parameter in both (1) and (2), presenting the possibility to test the description given above by performing simulations at different temperatures. In this work we compare the data for $T_0 = 0$ K, shown in Fig. 1a, with simulation results for $T_0 = 500$ K, Fig. 1b. Qualitatively, the yield–fluence dependencies for two different temperatures are similar. In both cases there are two regimes of molecular ejection separated by threshold fluences. The value of the ablation threshold fluence, $F_{th}$, however, is different for the two sets of simulations with $\sim 33\%$ lower threshold for simulation with $T_0 = 500$ K. Applying (1) and (2) to describe the simulation data, we found that the same activation energies $E_s^*$ and $E_v^*$, obtained from the fits to the data for zero temperature simulations, provide a good representation of the simulation data for $T_0 = 500$ K. This quantitative agreement between simulation results with different initial temperatures does support the description of the yield–fluence dependence given by (1) and (2) as well as the underlying physical mechanisms of molecular ejection.

A linear decrease in the detection threshold with increasing sample temperature has been experimentally observed for both neutral molecules and ions [5]. The detection threshold for neutral molecules in mass spectrometry experiments can be related to the lowest laser fluences at which a noticeable number of molecules desorb from the irradiated surface in the simulations ($\sim 15$ J/m$^2$ at $T_0 = 0$ K and $\sim 5$ J/m$^2$ for $T_0 = 500$ K). The detection threshold for ions is more difficult to relate to the simulation data. We can speculate, however, that, since both threshold fluences and yield–fluence dependencies for matrix ions and analyte molecules in MALDI are nearly identical [3], it is plausible to relate the detection threshold for matrix ions and analyte molecules to the ablation threshold, $F_{th}$, in the simulations ($\sim 35$ J/m$^2$ at $T_0 = 0$ K and $\sim 25$ J/m$^2$ for $T_0 = 500$ K). Indeed, the large analyte molecules in MALDI are unlikely to be ejected through the thermal desorption from the surface and their ejection should involve entrainment into the plume of ejected matrix molecules [12, 22, 23]. The linear dependence of the detection threshold on sample temperature observed experimentally for neutral molecules [5] agrees with (1) for thermal desorption. On the other hand, (2) for ablation also predicts a linear dependence of the ablation threshold on temperature, $F_{th} = L_p(E_v^* - CT_0)$, which could be related to the observed linear dependence of the detection threshold for matrix ions.

Another observation from the simulations that implies caution against straightforward interpretation of mass spectrometry experimental data is that the yield of monomers does not reflects the total amount of material ejected in the ablation regime. Moreover, the drastic increase of the total yield at the ablation threshold is imperceptible in the fluence dependence of the monomer yield. This can be seen in Fig. 3, where Arrhenius plots of the yield of monomers are shown for simulations with two initial temperatures. Only detection thresholds, but not ablation thresholds, can be identified from these plots. We find that (1) can provide a relatively good description of the monomer yield for both initial temperatures with the same value of activation energy, $E_s^* = 0.52$ eV, but a somewhat different pre-exponential factor. This observation agrees with

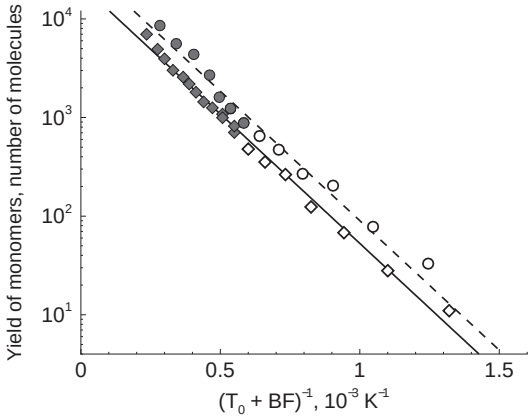


**Fig. 3.** Arrhenius plots of the yield of monomers from simulations with two initial temperatures. The *diamonds* and *circles* represent the data points for $T_0 = 0$ K and $T_0 = 500$ K, respectively. The *open* and *closed symbols* show the data points below and above the threshold for ablation. The *solid* and *dashed lines* represent fits of the data for $T_0 = 0$ K and $T_0 = 500$ K to the thermal desorption model (1) with the same activation energy of 0.52 eV

the results in [3] and [5], where the thermal desorption model is used to describe mass spectrometry experimental data over the whole range of fluences. While providing a seemingly good fit of the monomer yield, the desorption model does not give a correct description of the ejection mechanism at high fluences, where collective ejection or ablation occurs.

### *2.2 Thermal confinement and stress confinement regimes of laser ablation: pulse duration dependence of the ejection mechanism*

In the discussion of the simulation results given in the previous subsection, the ejection process is related to the amount of energy supplied by the laser pulse and to the distribution of the energy within the sample. In other words, in the regime of thermal confinement, when dissipation of the absorbed laser energy by thermal conduction can be neglected, the amount of ejected material and the transition between the ejection regimes is assumed to be completely defined by laser fluence, initial temperature and absorption coefficient, as can be seen from (1) and (2). There are, however, experimental observations suggesting that the rate of energy deposition can be an important factor. In particular, massive material removal or laser damage has been reported to occur at the energy densities much lower than those required for boiling and vaporization [18–20, 24, 25]. A plausible explanation for the onset of "cold" laser ablation has been proposed based on consideration of photomechanical effects caused by laser-induced stresses [19, 26]. It has been discussed that the magnitude of the laser induced stresses and the role of the associated photomechanical effects in material removal becomes significant when the laser pulse duration, $\tau_p$, is shorter than the time of mechanical equilibration of the absorbing volume, $\tau_s$ [18–20, 24, 25]. This condition, usually referred as inertial [14, 19] or stress confinement [20, 24, 25], can be expressed as $\tau_p \leq \tau_s \sim L_p/C_s$, where $C_s$ is the speed of sound in the irradiated material.

In order to investigate the dependence of the ablation process on the laser pulse duration, we perform, in addition to

the simulations with 150-ps pulses described above, a series of simulations with shorter pulse duration of 15 ps. Using the same penetration depth of 50 nm in both series of simulations, we ensure that the regimes of thermal and stress confinement are realized for 150 ps and 15 ps pulses, respectively. Below we give only a short comparison of the ablation process in the two irradiation regimes. More detailed analysis will be presented in a separate paper [27].

A mere visual inspection of the snapshots from the simulations performed with 150-ps laser pulses (Fig. 4a,b) and 15-ps laser pulses (Fig. 4c) reveal several important differences between the ablation mechanisms in the thermal and stress confinement regimes.

First, the threshold fluence for the ablation onset is significantly (by 22% [27]) lower for irradiation with 15-ps pulses than for 150-ps pulses. This difference can be illustrated by the snapshots shown in Fig. 4a and 4c. Although the laser fluence is smaller in the simulation shown in Fig. 4c, a large amount of material is ejected in this case, whereas the molecular ejection in Fig. 4a is limited to the intense evaporation from the surface. In other words, ablation is observed in the simulation illustrated by Fig. 4c, whereas the simulation in Fig. 4a is still in the desorption regime.

Second, the snapshot in Fig. 4c clearly shows that the mechanism of material ejection in this case is rather different from the homogeneous phase explosion responsible for the ablation onset in the regime of thermal confinement and illustrated by Figs. 2 and 4b. We found that the condition of stress confinement, realized in simulations with 15-ps laser pulses, results in the buildup of a high pressure within the absorbing region during the laser pulse. Interaction of the laser-induced pressure with free surface leads to the development of the tensile stresses that reach their maximum at a certain depth under the surface and can cause mechanical fracture or spallation (Fig. 4c). The spallation proceeds through nucleation and growth of voids/microcracks within the spallation region [27]. Snapshots from our earlier two-dimensional simulations (Fig. 5) can provide a molecular-level illustration of the difference between laser damage localized in the spallation region and homogeneous decomposition due to the overheating.

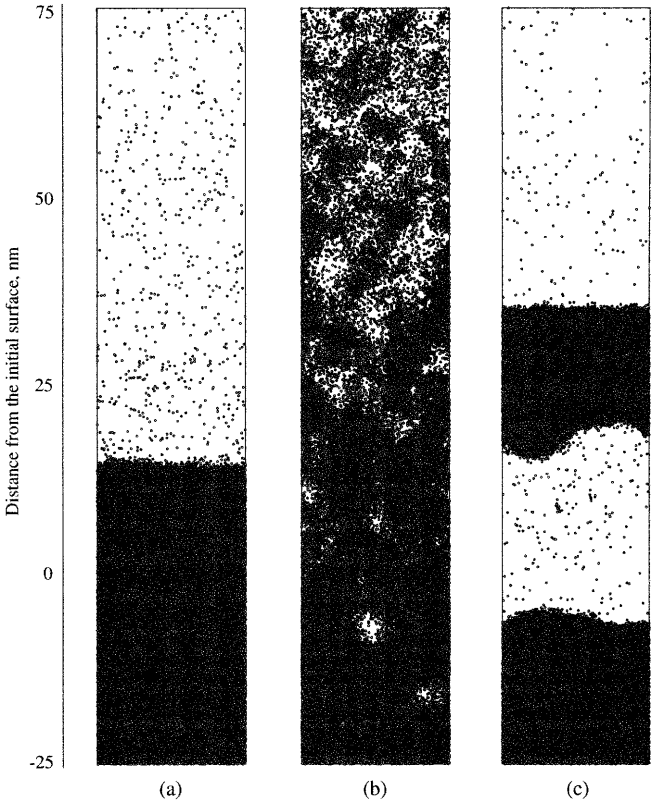


**Fig. 4a–c.** Snapshots from the simulations in the desorption (**a**) and ablation (**b**,**c**) regimes. The laser pulse durations are 150 ps (**a**,**b**) and 15 ps (**c**), fluences are 34 J/m$^2$ (**a**), 55 J/m$^2$ (**b**) and 31 J/m$^2$ (**c**). The laser penetration depth is 50 nm in all simulations. The irradiation parameters correspond to the regime of thermal confinement in **a** and **b** and to the regime of stress confinement in **c**

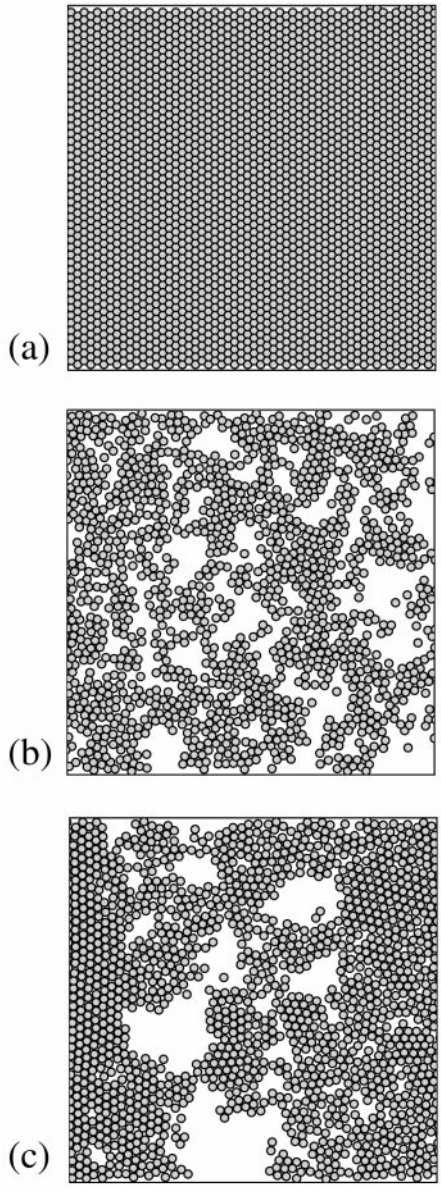


**Fig. 5a–c.** Snapshots from two-dimensional simulations that provide molecular level pictures of **a** initial two-dimensional configuration before irradiation with laser pulse, **b** homogeneous decomposition of irradiated material due to the phase explosion and **c** heterogeneous photomechanical disintegration. The laser irradiation is directed from the right side of the pictures

Third, it is apparent from the snapshots shown in Figs. 4 and 5 that much bigger and colder clusters can be ejected in the stress confinement regime as compared to the thermal confinement regime. From Fig. 4c we can only conclude that the size of the ejected chunk of material is bigger than the size of the computational cell used in the simulation. The sizes of the liquid droplets observed in simulations with 150-ps pulses are always smaller than the size of the computational cell. The ejection of small, sub-micron-sized particles under UV MALDI conditions has indeed been observed in recent trapping plate experiments by Handschuh et al. [23]. The fluence dependence of the particle ejection observed in [23], namely, no particle ejection below the ablation threshold, appearance of particles right above the threshold and decreased particle ejection at higher laser fluences, is consistent with simulation results [13, 14]. Indirect evidence of the ejection of molecular clusters has been also obtained in post-ionization time-of-flight mass spectrometry experiments by Hankin and John [28]. The ejection of larger clusters in the regime of stress confinement could be relevant to IR MALDI experiments, for which no data on cluster ejection is available yet.

## 3 Summary

The results of simulations performed for two initial temperatures and a wide range of laser fluences provide a consistent physical picture of laser desorption and ablation of molecular systems. At low laser fluences, thermal desorption from the surface is observed. The desorption yield consists primarily of monomers and can be well described by an Arrhenius-type dependence on the laser fluence. The same activation energy describes the desorption yield in simulations with different initial temperatures. At fluences above a certain threshold fluence, collective multilayer ejection or ablation occurs and the ablation depth follows a critical density of the deposited energy. The temperature dependence of the threshold fluence and the ablation yield is found to be consistent with this description, with the critical energy density being independent of the initial temperature.

The yield of monomers measured in mass spectrometry experiments appears to be not sensitive to the drastic increase of the total yield at the ablation threshold. The ablation threshold cannot be identified from the fluence dependence of the monomer yield, which deceptively follows an Arrhenius-type dependence even in the high-fluence region, where ablation occurs. In general, simulation results demonstrate that mechanistic interpretation of mass spectrometry data can be misleading. An extensive experimental study involving simultaneous detection of analyte and matrix molecules/ions as well as clusters of matrix molecules for a wide range of laser fluences is needed to ensure a reliable interpretation of experimental data and to clarify the mechanisms of molecular ejection.

The mechanism of material removal in the ablation regime depends strongly on the pulse duration. With longer laser pulses, in the regime of thermal confinement, phase explosion of the overheated material leads to the ejection of liquid droplets and gas phase molecules. With shorter pulses or larger penetration depths there is stress confinement, and high thermoelastic pressure can cause mechanical fracture or spallation. In this case material disintegration is localized within the spallation region leading to the onset of massive material removal at lower laser fluences and to the ejection of larger and colder molecular clusters as compared to the ablation in the regime of thermal confinement.

*Acknowledgements.* We gratefully acknowledge financial support from the Office of Naval Research through the MFEL Program. The computational support for this work was provided by the IBM-SUR Program and the Center for Academic Computing at Penn State University. We thank Klaus Dreisewerd and Franz Hillenkamp for insightful and stimulating discussions and Gareth Williams for reading the manuscript in the preparation stage and making useful suggestions.

## References

1. S.L. Jacques (Ed.): *Laser–Tissue Interaction IX*, SPIE Proc. Series, Vol. 3254 (SPIE, Washington DC 1998)
2. J.C. Miller, R.F. Haglund, Jr. (Eds): *Laser Ablation and Desorption* (Academic Press, London 1998)
3. K. Dreisewerd, M. Schürenberg, M. Karas, F. Hillenkamp: Int. J. Mass Spectrom. Ion Processes **141**, 127 (1995)
4. K. Dreisewerd, M. Schürenberg, M. Karas, F. Hillenkamp: Int. J. Mass Spectrom. Ion Processes **154**, 171 (1996)
5. M. Schürenberg, K. Dreisewerd, S. Kamanabrou, F. Hillenkamp: Int. J. Mass Spectrom. Ion Processes **172**, 89 (1998)
6. A. Vertes, R. Gijbels: *Laser Ionization Mass Analysis*, ed. by A. Vertes, R. Gijbels, F. Adams (John Wiley, New York 1993) p. 127
7. R. Srinivasan, B. Braren: Chem. Rev. **89**, 1303 (1989)
8. S.M. Metev, V.P. Veiko: *Laser-assisted microtechnology* (Springer, Berlin 1998)
9. A. Bencsura, A. Vertes: Chem. Phys. Lett. **247**, 142 (1995)
10. A. Bencsura, V. Navale, M. Sadeghi, A. Vertes: Rapid Commun. Mass Spectrom. **11**, 679 (1997)
11. £. Dutkiewicz, R.E. Johnson, A. Vertes, R. Pędrys: J. Phys. Chem. A **103**, 2925 (1999)
12. L.V. Zhigilei, P.B.S. Kodali, B.J. Garrison: J. Phys. Chem. B **101**, 2028 (1997); ibid., **102**, 2845 (1998)
13. L.V. Zhigilei, B.J. Garrison: Appl. Phys. Lett. **74**, 1341 (1999)
14. L.V. Zhigilei, P.B.S. Kodali, B.J. Garrison: Chem. Phys. Lett. **276**, 269 (1997)
15. L.V. Zhigilei, B.J. Garrison: Appl. Surf. Sci. **127-129**, 142 (1998); ibid., In *Laser–Tissue Interaction IX*, SPIE Proc. Series 3254, 135 (1998)
16. L.V. Zhigilei, B.J. Garrison: Mater. Res. Soc. Proc. **538**, 491 (1999)
17. L.V. Zhigilei, B.J. Garrison: Proc. Int'l. Conf. on Modeling and Simulation of Microsystems, Semiconductors, Sensors, and Actuators, 138 (1999)
18. R. Cramer, R.F. Haglund Jr., F. Hillenkamp: Int. J. Mass Spectrom. Ion Processes **169**/**170**, 51 (1997)
19. I. Itzkan, D. Albagli, M.L. Dark, L.T. Perelman, C. von Rosenberg, M.S. Feld: Proc. Natl. Acad. Sci. USA **92**, 1960 (1995)
20. A.A. Oraevsky, R. Esenaliev, S.L. Jacques, F.K. Tittel: SPIE Proc. **2391**, 300 (1995)
21. R. Kelly, A. Miotello: Appl. Surf. Sci. **96-98**, 205 (1996)
22. L.V. Zhigilei, B.J. Garrison: Appl. Phys. Lett. **71**, 551 (1997); ibid., Rapid Commun. Mass Spectrom. **12**, 1273 (1998)
23. M. Handschuh, S. Nettesheim, R. Zenobi: Appl. Surf. Sci. **137**, 125 (1999)
24. G. Paltauf, H. Schmidt-Kloiber: Appl. Phys. A **62**, 303 (1996)
25. S.L. Jacques, A.A. Oraevsky, R. Thompson, B.S. Gerstman: SPIE Proc. **2134**A, 54 (1994)
26. R.S. Dingus, R.J. Scammon: SPIE Proc. **1427**, 45 (1991)
27. L.V. Zhigilei, B.J. Garrison: in preparation
28. S.M. Hankin, P. John: J. Phys. Chem. B **103**, 4566 (1999)